Giant, 19, 2024, 100316

Full-length article

Chiral ferroelectric nematic liquid crystals as materials for versatile laser devices

César L. Folcia [a,*], Josu Ortega [a,*], Teresa Sierra [b], Alejandro Martínez-Bueno [b], Jesús Etxebarria [a]

[a] Department of Physics, Faculty of Science and Technology, University of the Basque Country, UPV/EHU, Bilbao, Spain
[b] Instituto de Nanociencia y Materiales de Aragón (INMA), Departamento de Química Orgánica, Facultad de Ciencias, CSIC-Universidad de Zaragoza, 50009 Zaragoza, Spain

Keywords: **Nematic ferroelectric liquid crystals, Liquid crystal lasers, Electrical tuning**

We present a liquid-crystal laser device based on the chiral ferroelectric nematic phase (N_F^*). The laser medium is obtained by mixing a ferroelectric nematic material with a chiral agent and a small proportion of a fluorescent dye. Notably, in the N_F^* phase very low electric fields perpendicular to the helical axis are able to reorient the molecules, giving rise to a periodic structure whose director profile is not single harmonic but contains the contribution of various Fourier components. This feature induces the appearance of several photonic bandgaps whose spectral ranges depend on the field, which can be exploited to build tunable laser devices. Here we report the characterization of home-made N_F^* lasers that can be tunable under low electric fields and present laser action in two of the photonic bands of the material. The obtained results open a promising route for the design of new and more versatile liquid-crystal based lasers.

1 Introduction

Photonic materials are periodic dielectric structures which show wavelength ranges where the propagation of some electromagnetic waves is forbidden. These spectral regions are called photonic band gaps (PBGs), and at their edges, the density of optical states shows a sharp increase. The high values of the density of states can be exploited for many applications including light amplification, leading to the so-called distributed feedback (DFB) laser action. Cholesteric liquid crystals (CLCs) are the most prominent examples of photonic materials among mesogenic compounds. They are constituted by chiral molecules that self-assemble forming a helical structure with a certain helical pitch. In these materials, it can be shown that a PBG results for circularly polarized light with the same handedness as that of the helix, which cannot propagate along the helix axis for a spectral region between $\lambda_o = pn_o$ and $\lambda_e = pn_e$, being p the helical pitch, and n_o and n_e the ordinary and extraordinary local refractive indices respectively. Hence, a mirrorless DFB type laser emission can be achieved at the short-wavelength edge (SWE) or long wavelength edge (LWE) of the gap when CLCs are doped with fluorescent dyes whose emission spectra overlap with the PBG [1-5]. Since the discovery of laser emission in CLCs by Kopp et al. in 1998 [1], many efforts have been made to build up CLC lasers with increasing performance, opening an extensive research field. This type of lasers presents useful characteristics, such as low pumping power threshold and ease of implementation in small devices. On the other hand, one of the most attractive features of photonic CLC lasers is the possibility of tuning the PBG by external stimuli, with the consequent shift of the emission wavelength. Examples of different external agents for laser tuning are light irradiation [6-9], temperature variation [10,11], or mechanical stretching [12].

* Corresponding authors.
E-mail addresses: cesar.folcia@ehu.es (C.L. Folcia), josu.ortega@ehu.es (J. Ortega).
Received 29 April 2024; Received in revised form 13 June 2024; Accepted 24 June 2024

https://doi.org/10.1016/j.giant.2024.100316

Especially interesting is the electric-field-induced tuning [13-17], since electric fields can be easily applied to the liquid crystal materials within the laser devices. Some examples of LC lasers tunable by electric fields are based on the oblique heliconical CLC (CLC_{OH}) state that certain CLCs display [18,19]. In these materials, the tuning can be driven by the strength or by the frequency of the electric field. Although the tuning range of the PBG is very wide in both cases, the molecular director makes an acute angle with the helix axis. This fact gives rise to a small contrast of the dielectric modulation of the structure, which produces an important decline of the density of states at the edges of the PBG and consequently a poor performance of the laser. A different approach of tunable lasers under applied field uses complex cells with polymer CLC mirrors whose pitch can be changed [20].

In the present work, we present a tuning alternative using a laser device based on the ferroelectric nematic (N_F) phase recently discovered [21-30]. Usually, this phase becomes stable when cooling the ordinary nematic phase N, although it can also appear directly from the isotropic liquid [31]. In the N_F phase the head-to-tail molecular invariance, characteristic of traditional LCs, is broken, giving rise to the appearance of a high macroscopic polarization (of the order of $\mu C/cm^2$) along the molecular director. Giant dielectric constants (of the order of 10^4) [32] and a high non-linear optical susceptibility (of the order of 10 pm/V) [33] are also remarkable features of these materials. Moreover, a chiral version of the N_F phase, the so-called chiral ferroelectric nematic phase (N_F^*), can be obtained by adding a small proportion of chiral component to the N_F material [34-36] or by slight chiral modifications in the chemical structure of those prototype molecules [37,38].

The linear optical properties of the N_F^* phase are the same as those of a N* structure (i.e. conventional CLC). This is true even though the actual periodicity is equal to the pitch p for the N_F^* structure and to $p/2$ for CLCs, due to the head-to-tail invariance of the molecular director in the latter case. Therefore, the N_F^* phase (as well as the CLC) shows a single selective reflection band at normal incidence centered at $\lambda = pn$, being λ the vacuum wavelength of light and $n = \sqrt{(n_e^2 + n_o^2)/2}$ the mean refractive index, in the usual way. The periodicity p of the N_F^* structure becomes evident, however, when an electric field is applied perpendicular to the helical axis. Upon field application the nematic director is reoriented according to the polarity of the field, favoring regions where the local polarization tends to be parallel to it, to the detriment of others where they are almost antiparallel [34-36]. As a consequence, the structure with periodicity p cannot be described by a single-harmonic modulation but also contains distortions whose Fourier components have periodicities p/m ($m = 2,\ 3,\ \ldots$). Therefore, a reflection band at $\lambda = 2pn$ appears together with bands centered at $\lambda_m = 2pn/m$ with reflectivity depending on the specific shape of the distortion and the relative magnitude of their Fourier contributions. On the other hand, the electric field can induce an enlargement of the pitch as has been shown in Refs. [34-36]. This electrical tuning of p depends on many factors, but a model that accounts for the main features of the phenomenon can be easily understood if we assume a weak anchoring of the director on the substrates. Under these conditions, we simply need to consider the elastic twist energy and the ferroelectric interaction with the electric field. The ferroelectric term tends to align the polarization parallel to the field and, consequently, there are regions where the elastic twist energy shows a significant increase. This energy increase can then be reduced if the director on the surfaces rotates in the opposite direction to the helical twist, thus increasing the pitch. In general, if the applied field is smaller than the critical field for helix unwinding, the profile of the director across the cell is complicated and exhibits many Fourier components of periodicities p/m ($m = 1,2,3\ldots$) with significant amplitudes. In the Supporting Information a more detailed explanation is presented. Recently, the opposite limit of strong anchoring conditions has also been studied experimentally [39], and the director profile has been analyzed numerically, finding also a behavior of the helix unwinding process totally different from that of ordinary CLC phases. Anyway, for our tuning purposes, the important point is that the increase in p gives rise to a redshift with the field in all the reflection bands. In summary, contrary to the case of the CLC_{OH} where a single band centered at $\lambda_2 = pn$ appears [18,19], the reflectance spectrum of the N_F^* structure under field shows various PBGs whose position, intensity, and shape depend on the applied field intensity.

Here, we report for the first time laser emission in a liquid crystal cell in the N_F^* phase. The study covers laser emission characteristics, electric-field-induced tuning at the LWE of the λ_2 photonic band (the only one observed without field), and lasing at the third harmonic λ_3 band of the distorted helical structure.

2 Experimental section

RM734 was synthetized following the procedure described in reference [33]. S1 was previously described in reference [37] and was synthetized for this work following a modified procedure gathered in the Supporting Information.

The temperature of the samples during texture analysis, reflectance spectroscopy, and laser emission experiments was controlled with a hot stage INSTEC SC-200 with 0.1 °C accuracy. Home-made plane-parallel cells, made of two glasses treated with polyvinyl alcohol and rubbed for parallel alignment, were prepared. The cells were capillary-filled in the isotropic phase. ITO strip electrodes separated 5 mm apart were patterned on one of the glasses for the application of in-plane electric fields. The sample gap was selected in a range $18 - 20\ \mu m$, which is typically the optimum thickness to minimize the threshold energy of the laser [40]. Texture observation together with analysis of the electrooptic behaviour under AC voltages at 0.5 Hz frequency were performed with a polarizing microscope (Olympus BX51). Spectroscopic measurements in the N_F^* phase were carried out in the reflection mode with a fiber-optic spectrometer (Avantes – AvaSpecULS2048-USB2, grating: 300 lines/mm, slit size =100 μm) with $\Delta\lambda = 5$ nm of resolution full width at half maximum (FWHM), using light from a deuterium-halogen lamp.

For laser experiments, cells were optically pumped by using a Nd:YAG laser (LOTIS TII LS-2138T-100), operating at the second harmonic frequency (wavelength 532 nm). The laser pulse duration was 14 ns with repetition rates of 0.5 or 1 Hz for different experiments and its intensity was selected with a variable reflectance type attenuator (LOTIS II Attenuator 532 nm). Laser

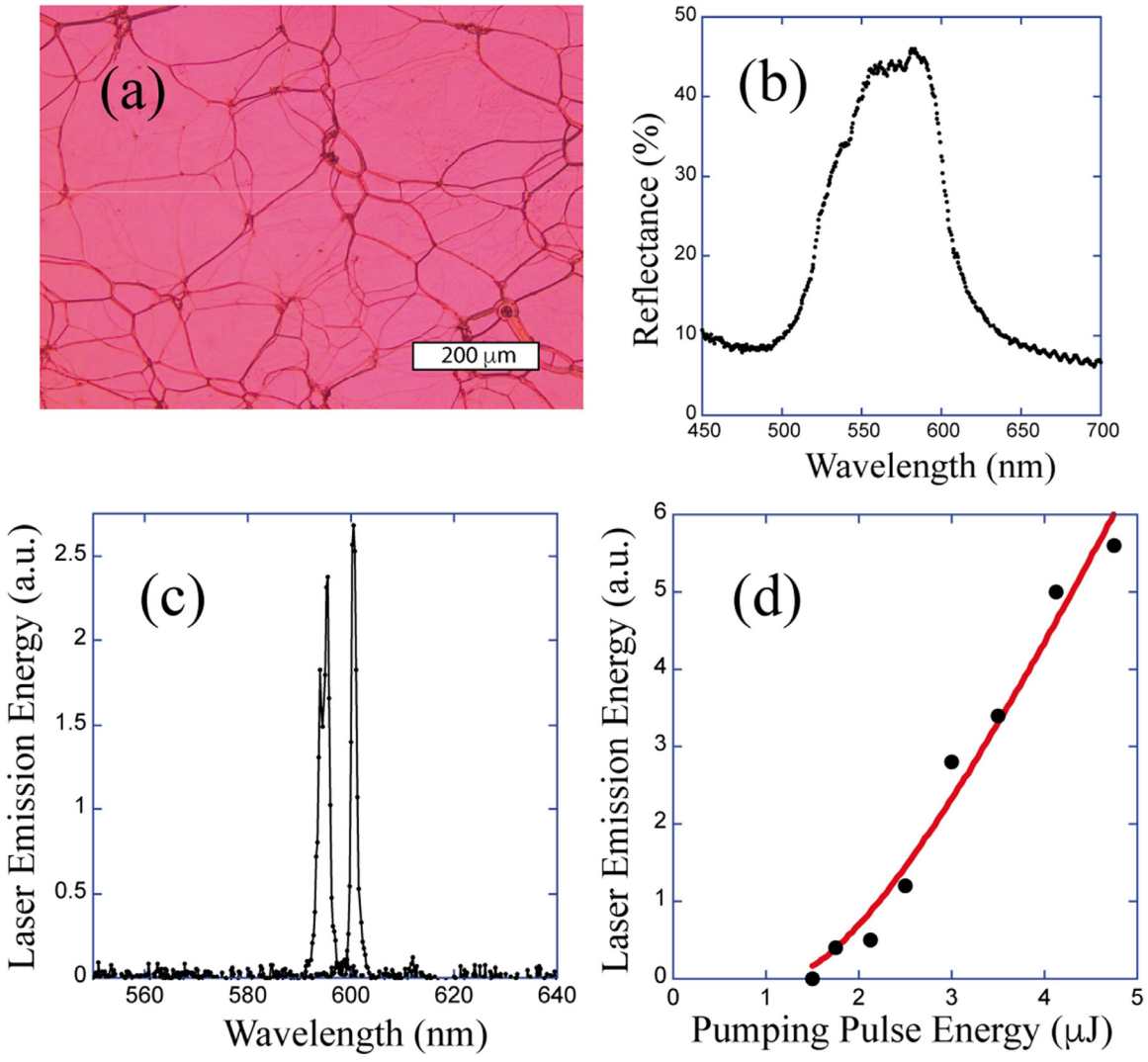

Fig. 1

Optical characteristics and laser emission at the LWE of the reflection band under zero field. (a) Photomicrograph of the texture of the material at 108 ºC in the N_F^* phase as observed between crossed polarizers. (b) Reflectance spectrum of the sample at the same temperature. (c) Laser emission spectra at two different regions of the cell when the material was optically pumped with 3 μJ/pulse. (d) Laser emission energy (in arbitrary units) vs energy of the pumping pulse.

light was right (or left) circularly polarized with a variable circular polarizer for 532 nm (Thorlabs VC5–532/M) before being focused on the sample, at normal incidence, with a lens of 20 cm of focal length. Pumping pulse energy was measured with a power meter (Ophir), at a repetition rate of 20 Hz. Laser pulses and square-wave electric field applied to the material were synchronized and their relative delay was controlled. A 532 nm notch filter was placed behind the sample to remove the pumping laser light. Laser emission spectra were measured using a fiber-based spectrometer (AvaSpec 2048) with a resolution of 0.4 nm FWHM whose optical fiber was situated just behind the notch filter without any focusing lens.

3 Experimental results and discussion

The material employed in the experiments was a mixture of the N_F liquid crystal 4-[(4-nitrophenoxy)carbonyl]phenyl2,4-dimethoxybenzoate (RM734) [21], the fluorescent dye 1,3,5,7,8-pentamethyl-2,6-di-t-butylpyrromethene-difluoroborate complex (PM597) (Sigma-Aldrich), and a chiral dopant to promote the helical structure. The type and proportion of the chiral dopant were selected in such a way that the PBG of interest was within the fluorescence range of the dye and, on the other hand, the local birefringence $\Delta n = n_e - n_o$ of the medium was reduced as little as possible, in order to preserve the contrast that defines the pitch periodicity. The material was aligned in the Cano geometry, i.e., with the helical axis perpendicular to the cell glasses and to the electric field. In all the cases the alignment was improved by applying low frequency (1 Hz) small AC voltages (~10 V) in the N_F^* phase for several minutes.

First, the usual laser emission was checked and characterized at the LWE of the reflection band of the N_F^* phase under zero field. We used a right-handed, chiral dopant: (13bS)−5,6-Dihydro-5-(trans-4-propylcyclohexyl)−4H-dinaphtho[2,1-f:1′,2′-h][1,5]dioxonin (R5011) (BLDpharm). RM734, R5011, PM597 were mixed in proportion 96.4:2.8:0.8 respectively (wt.%). Although the chemical structures of RM734 and R5011 are

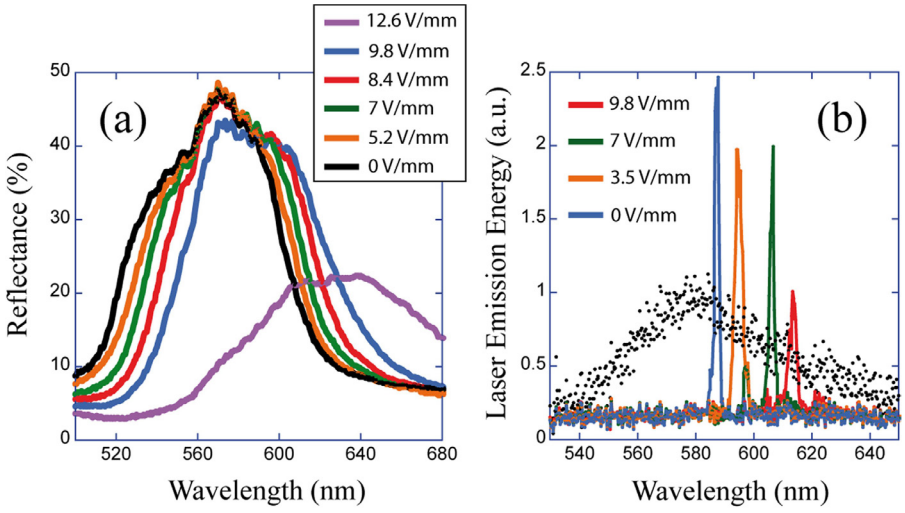

Fig. 2

Electrically induced tuning. (a) Time averaged reflectance spectra around the λ_2 photonic band measured for different square-wave electric field intensities of frequency 10 Hz. The structure becomes strongly distorted for fields higher than about 11 V/mm. (b) Laser emission spectra for different square-wave electric fields of frequency 1 Hz. Black points represent the fluorescence spectrum of the dye, and are drawn on a different scale.

quite different, we found no incompatibility in the resulting mixtures given the low proportion of chiral component. With these concentrations the N_F^* phase becomes stable at 120 ºC on cooling from the high temperature N* phase, and undergoes a transition to a crystalline solid phase at about 90 ºC. Fig. 1(a) shows a typical texture of the sample in the N_F^* phase as observed between crossed polarizers. Oily streak defects are present in the texture which is in detriment of the laser performance. However, tuning of the PBG is only possible with not too strong surface anchoring [34,36] and, perhaps, this is the reason why more homogeneous texture could not be obtained. Fig. 1(b) represents the reflectance spectrum of the sample. In spite of the fact that the alignment was far from being ideal, laser emission was detected when the cell was optically pumped. The pumping light was left-handed circularly polarized, in order to optimize the excitation conditions, with a pulse energy of 3 μJ and a repetition rate of 1 Hz. The light was focused on the cell at normal incidence and the spot was Gaussian, with a diameter D4σ = 240 μm (FWHM = 144 μm). Fig. 1(c) shows the laser emission observed when focusing on two different regions of the sample. A slight difference in the laser wavelength is detected due to small inhomogeneities in the pitch values across the sample area, which are more sensitive to sample thickness variations than usual CLCs.

Black circles in Fig. 1(d) represent the laser emission energy (in arbitrary units) for various pumping pulse energies. They show the typical dependence of a laser emission, i.e., a threshold energy from which the emission intensity grows almost linearly with the pumping intensity.

Taking into account the Gaussian profile of the illumination spot, it can be shown [5] that the energy emitted as laser radiation, E_{laser}, is related to the input energy E_{in} according to the expression

$$E_{laser} = C\left[E_{in} - E_{th}\left(1 + \ln\frac{E_{in}}{E_{th}}\right)\right], \quad (1)$$

where E_{th} is the threshold energy and C is a constant related to the slope efficiency for $E_{in} >> E_{th}$. From a fit of the experimental points in Fig. 1(d) to expression (1) (red line) the parameters $C = 2.9 \pm 0.3$ and $E_{th} = 1.1 \pm 0.1$ μJ/pulse result. It is interesting to point out that E_{th} is comparable to typical threshold energies of conventional CLC lasers. The constant C is not relevant in the present study since E_{laser} is expressed in arbitrary units. For example, $E_{th} = 1.2 \pm 0.1$ μJ/pulse was reported in reference [5] for a sample of 10 μm thickness with the same dye. Although E_{th} should certainly increase somewhat for thinner samples, it seems that the performance of the laser based on the N_F^* phase of the RM734 – R5011 mixture is quite acceptable despite its alignment imperfections.

Next, a square wave electric field of frequency 10 Hz was applied to the material. Fig. 2(a) represents the selective reflection band corresponding to $\lambda_2 = pn$ for different field intensities. As a consequence of the pitch enlargement, the zero-voltage band is gradually (and reversibly) red shifted when the field is increased. The typical response times are always much smaller that the driving field and pumping period. For electric fields higher than about 11 V/mm the reflectance spectrum rapidly decreases and becomes less defined, indicating a significant distortion of the structure. Under the polarizing microscope the sample texture undergoes just a slight color variation in the regime of small fields we have used. Larger fields however produce more complicated nucleation processes that ultimately lead to the helix unwinding. Fig. 2(b) shows laser emissions observed for different square-wave electric fields of frequency 1 Hz. The pumping laser was synchronized with the square voltage and was triggered with a delay of 0.1 s after the polarity inversion to ensure completion of the distortion process while reducing as much as possible the unavoidable shielding due to the migration of electrical charges from impurities. A typical profile of the laser spot is shown in the Supporting Information (Fig. S8). As in the spectra of Fig. 2(a), the electric field was varied monotonously and the effect was

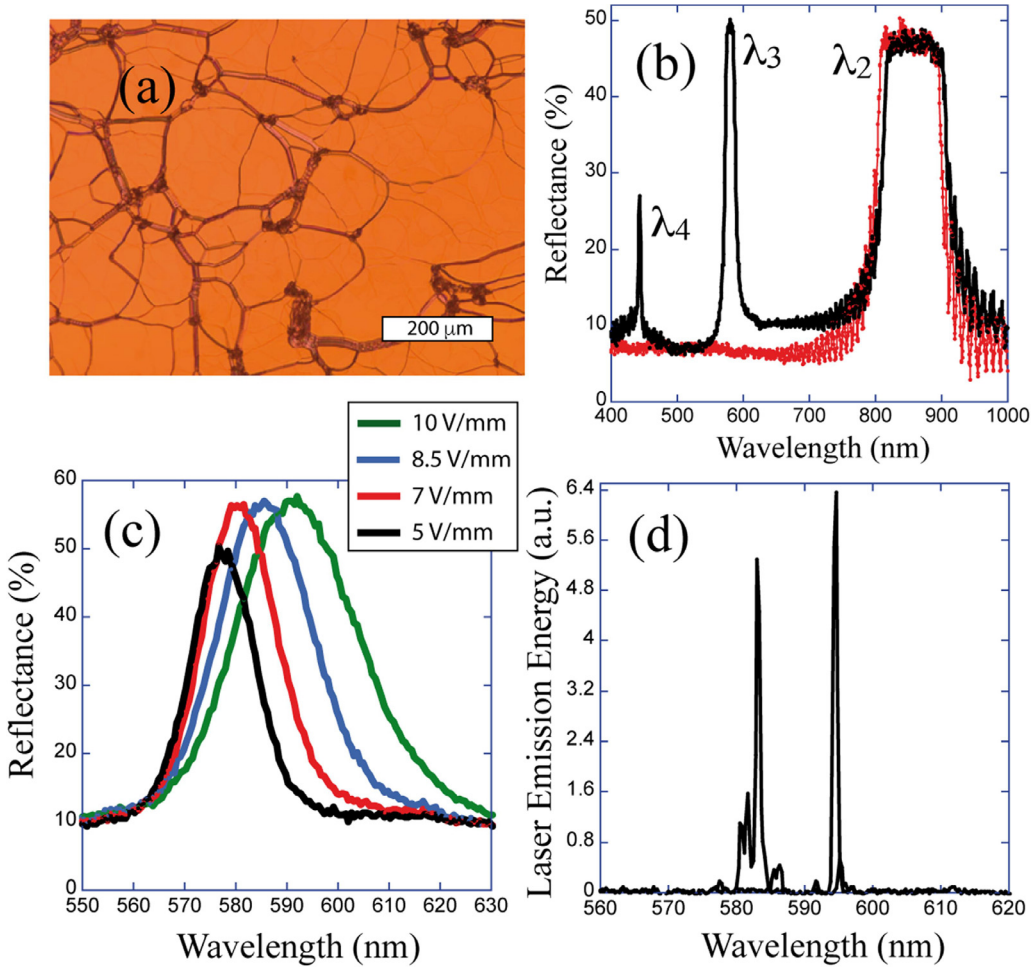

Fig. 3

Optical characteristics and electric-field tuning of the λ_3 band. (a) Photomicrograph of the texture of the material at 104 ºC in the N_F^* phase as observed between crossed polarizers. (b) Reflectance spectrum under zero field (red line) and for a square-wave electric field intensity of 7 V/mm and frequency 10 Hz (black line). The different photonic bands for $m = 2,\ 3$, and 4 are indicated. The full pitch band $m = 1$ is not represented in the figure since it is placed in the infrared region, out of our spectral detection range. (c) Reflectance spectra around the λ_3 photonic band measured for different square-wave electric field intensities of frequency 10 Hz. (d) Single-shot laser emission spectra at two different regions of the cell when the material was optically pumped with 8 μJ/pulse and repetition rate 1 Hz, synchronized with an applied square-wave electric field of 7 V/mm.

found to be reversible although, for relatively high fields, the material requires to remain at zero field for a certain time (about 1/2 min) to recover the initial condition. Fig. 2(b) shows also the fluorescence spectrum of the dye in the material (black dots). The laser intensity reduces as the dye fluorescence decreases. Note there is no way to achieve tunability while maintaining uniform laser intensity unless the pumping power is modified. This is a common phenomenon for all kinds of tunable lasers. However, the tuning range is not only limited by the fluorescence range but also by the electric field intensity, i.e., lasing is hardly possible if the field produces a significant structural distortion (see e.g. the PBG of Fig. 2(a) for 12.6 V/mm).

Finally, a different mixture was prepared in order to take the 3rd harmonic λ_3 band into the fluorescence range of the dye with the purpose of investigating the possibility of lasing emission at this photonic band. We used a different left-handed chiral dopant: 4-[(4-nitrophenoxy)carbonyl]phenyl (*S*)−2-(sec–butoxy)−4-methoxybenzoate (S1) [37], because the results with R5011 were not satisfactory probably due to a reduction of the local birefringence induced by the chiral dopant that becomes more relevant in the strength of the λ_3 band. Contrary to R5011, S1 is a chiral nematic ferroelectric liquid crystal below 40 ºC and was used by Zhao et al. [37] in mixtures with RM734 in different proportions to promote N_F^* phases with controlled pitch length. For our sample, we prepared a mixture of RM734, S1, PM597 in proportions 78.7:20.5:0.8 (wt.%). In this mixture the N_F^* phase becomes stable at 116 ºC on cooling from the high temperature N^* phase, and crystallization occurs at about 80 ºC. Fig. 3(a) shows the texture of the sample in the N_F^* phase as observed between crossed polarizers. As can be seen, some oily streaks are also present in similar proportion as those in the previous mixture and were also present in the N^* phase. Fig. 3(b) represents the reflection spectrum under zero field (red line) and the one observed when a square wave electric field of frequency 10 Hz and amplitude 7 V/mm was applied to the material (black line). In both cases, the usual $\lambda = pn$ band is clearly visible at 850 nm. This implies a helical

twisting power of about 10 μm^{-1} for S1 in RM734. Apart from the main gap, different λ_m photonic bands ($\lambda_m = 2pn/m,\ m = 3, 4$) are clearly visible when the field is applied ($\lambda_3 = 580$ nm and $\lambda_4 = 443$ nm in Fig. 3(b)). The full pitch photonic band gap is not depicted in the figure since its corresponding wavelength λ_1 lies in an infrared region out of the spectrometer detection range. These secondary gaps disappear if there is no applied field, with only the main gap λ_2 remaining. Fig. 3(c) represents the $m = 3$ band for different electric field amplitudes. For moderate fields, it is gradually and reversibly red shifted as a consequence of the pitch enlargement when the field is increased. The tuning amplitude for this band is approximately 2/3 of that of the zero-field one ($\lambda_2 = pn$). The relation is not exact because of index dispersion. Laser emission was attempted by optically pumping the material with right-handed circularly polarized light and repetition rate of 1 Hz, synchronized with the applied square-wave electric field. Fig. 3(d) shows two laser shots for a field-amplitude of 7 V/mm and a pumping energy of 8 μJ/pulse emitted from different regions of the sample. The small differences in the laser wavelength can be attributed to inhomogeneities in the sample pitch or in the electric field in the different regions of the sample. In this case, we could not further characterize this laser or evaluate its electrical tuning possibilities because lasing stops after a few pulses. We speculate that heating by such an energetic pumping beam can presumably induce changes in the N_F^* structure and also decompose the organic dye molecules at the illuminated spot region. A total recuperation of the laser performance requires a slow process involving molecular diffusion that replace the deteriorated molecules by new ones at the spot position. The low performance of lasing around λ_3 in comparison with the LWE of the λ_2 PBG was not completely unexpected because the density of states at λ_3 is smaller (see Supporting Information, Figs. S6-S7), and lasing must then require high pumping powers.

We would like to finish this section by pointing out that a substantial improvement in the performance of the lasers described here could be achieved with a better alignment of the N_F^* phase. In our opinion this is the main factor which limits in practice the laser performance in all the configurations examined. Good alignment enhances the quality factor of the laser cavity because reduces the scattering of the pumping light, which leads to the decrease of E_{th} and to the increase of the laser slope efficiency [41,42]. In this regard the knowledge we have on the alignment of helielectric nematics is still far from that of ordinary CLCs, for which there is an accumulated experience of tens of years. It would then be worthwhile to investigate the quality of alignment that can be achieved with other procedures (e.g., shearing), other aligning agents, or other N_F^* materials, some of which could work even at room temperature. Beside this, another interesting strategy to improve lasing is the use of multilayer cells [5,42], which, in its simplest configuration, consists of assembling three cholesteric layers of different handedness. The two external films have the same handedness as the active medium, are inactive and act as reflectors, and only the internal layer is dye-doped. Thus, the role of the reflectors is similar to that of the mirrors in Fabry-Perot cavity lasers. Using this strategy, a considerable reduction of E_{th} was achieved [5,42] in conventional CLC lasers, which could be very useful in the framework of the present work for lasing emission at the 3rd or 4th harmonic photonic bands.

4 Conclusions

We presented some laser devices based on the chiral ferroelectric nematic phase. We have demonstrated the possibility of attaining laser emission not only at the edges of the usual λ_2 half pitch PBG but also at the third harmonic band that appears when an electric field is applied perpendicular to the helical axis, and whose wavelength depends on the field intensity. In addition, we have shown the possibility of tunable laser emission at the LWE of the half pitch PBG under electric fields. The process is fully reversible and we have attained a tuning range of about 30 nm.

In order to check the laser quality, we have characterized the usual laser emission at zero field, and have observed similar thresholds as CLC based standard lasers. It is interesting to point out that very low electric fields (of the order of a few V/mm) are sufficient to induce structural distortions that result in relevant changes in the photonic properties of a N_F^* material. This greatly facilitates experiments, as well as the design of laser devices. In contrast to this, we reported previously laser emission at the second order PBG of the electrically-distorted helix of a conventional CLC [43]. In that case, electric field bursts of 20 kHz of frequency and 4500 V/mm were necessary to be applied during a short time (0.1 – 2 ms) in order to strongly distort the helix without unwinding it.

Evidently, we are still far from achieving a N_F^* laser for practical use. Further work is needed to understand the electrical tunability of the pitch, as well as to synthesize N_F^* phases that are stable at room temperature, exhibit good alignment properties and show larger tuning ranges. However, there are no fundamental impediments to overcoming all these issues, and the advantages that future N_F^* materials would present over conventional CLCs are obvious. We believe that the results we have presented here open up new and interesting possibilities for the use of helielectric nematics in the field of multi-wavelength liquid crystal lasers.

As a general conclusion, this work demonstrates some interesting possibilities of laser emission based on N_F^* materials. The rich variety of photonic properties exhibited by these materials makes them singular candidates to design simpler and versatile laser devices. These are some of our ideas for future work.

Declaration of competing interest

The authors declare that they have no known competing financial interests or personal relationships that could have appeared to influence the work reported in this paper.

Data availability

No data was used for the research described in the article.

CRediT authorship contribution statement

César L. Folcia: Conceptualization, Investigation, Writing – review & editing. **Josu Ortega:** Conceptualization, Investigation, Writing – review & editing. **Teresa Sierra:** Investigation. **Alejandro Martínez-Bueno:** Investigation. **Jesús Etxebarria:** Conceptualization, Investigation, Writing – review & editing.

Acknowledgments

This work was financially supported by the Basque Government project IT1458–22, the Spanish project PID2021–122882NB-I00/AEI /10.13039/501100011033/ and by "ERDF A way of making Europe", the Gobierno de Aragón-FSE (E47_23R- research group). The authors would like to acknowledge the Servicios Científico-Técnicos of CEQMA (CSIC-Universidad de Zaragoza) for their support.

Supplementary materials

Supplementary material associated with this article can be found, in the online version, at doi:10.1016/j.giant.2024.100316.

References

[1] V.I. Kopp, Z.Q. Zhang, A.Z. Genack, Lasing in chiral photonic structures, Prog, Quantum Electron. 27 (2003) 369–416.

[2] L.M. Blinov, R. Bartolino (Eds.), Liquid Crystal Microlasers, Transworld Research Network, Trivandrum, India, 2010.

[3] H. Takezoe, Liquid crystal lasers, in: Q. Li (Ed.), Liquid Crystals Beyond Displays, Wiley, Hoboken, NJ, 2012, pp. 1–28.

[4] H. Coles, S. Morris, Liquid-crystal lasers, Nat. Photonics 4 (2010) 676–685.

[5] J. Ortega, C.L. Folcia, J. Etxebarria, Upgrading the performance of cholesteric liquid crystal lasers: improvement margins and limitations, Materials (Basel) 11 (2018) 5.

[6] P.V. Shibaev, R.Lea Sanford, D. Chiappetta, V. Milner, A. Genack, A. Bobrovsky, Light controllable tuning and switching of lasing in chiral liquid crystals, Opt. Express 13 (2005) 2358–2363.

[7] G.S. Chilaya, Light-controlled change in the helical pitch and broadband tunable cholesteric liquid-crystal lasers, Crystallogr. Rep. 51 (2006) S108–S118.

[8] L.J. Chen, J.D. Lin, C.R. Lee, An optically stable and tunable quantum dot nanocrystal-embedded cholesteric liquid crystal composite laser, J. Mater. Chem. C 2 (2014) 4388–4394.

[9] T.V. Mykytiuk, I.P. Ilchishin, O.V. Yaroshchuk, R.M. Kravchuk, Y. Li, Q. Li, Rapid reversible phototuning of lasing frequency in dye-doped cholesteric liquid crystal, Opt. Lett. 39 (2014) 6490–6493.

[10] K. Funamoto, M. Ozaki, K. Yoshino, Discontinuous shift of lasing wavelength with temperature in cholesteric liquid crystal, Jpn. J. Appl. Phys. 42 (2003) L1523–L1525.

[11] Y. Huang, Y. Zhou, C. Doyle, S.T. Wu, Tuning the photonic band gap in cholesteric liquid crystals by temperature-dependent dopant solubility, Opt. Express 14 (2006) 1236–1242.

[12] H. Finkelmann, S.T. Kim, A. Muñoz, P. Palffy-Muhoray, B. Taheri, Tunable mirrorless lasing in cholesteric liquid crystalline elastomers, Adv. Mater. 13 (2001) 1069–1072.

[13] H. Yu, B.Y. Tang, J. Li, L. Li, Electrically tunable lasers made from electro-optically active photonics band gap materials, Opt. Express 13 (2005) 7243–7249.

[14] B. Park, M. Kim, S.W. Kim, W. Jang, H. Takezoe, Y. Kim, E.H. Choi, Y.H. Seo, G.S. Cho, S.O. Kang, Electrically controllable omnidirectional laser emission from a helical polymer network composite film, Adv. Mater. 21 (2009) 771–775.

[15] J. Schmidtke, G. Jünnemann, S. Keuker-Baumann, H.S. Kitzerow, Electrical fine tuning of liquid crystal lasers, Appl. Phys. Lett. 101 (2012) 051117.

[16] Y.-S. Lo, Y.-M. Liu, H.-C. Yeh, Low-voltage and wide-band tuning of lasing in a dye-doped liquid-crystal sandwich structure, Opt. Express 23 (2015) 30421–30428.

[17] J. Ortega, C.L. Folcia, J. Etxebarria, Liquid-crystal-based resonant cavities as a strategy to design low-threshold electrically-tunable lasers, Liq. Cryst. 49 (2022) 427–435.

[18] J. Xiang, A. Varanytsia, F. Minkowski, D.A. Paterson, J.M.D. Storey, C.T. Imrie, O.D. Lavrentovich, P. Palffy-Muhoray, Electrically tunable laser based on oblique heliconical cholesteric liquid crystal, Proc. Natl. Acad. Sci. U.S.A. 113 (2016) 12925–12928.

[19] B. Liu, C.-L. Yuan, H.-L. Hu, H. Wang, Y.-W. Zhu, P.-Z. Sun, Z.-Y Li, Z.-G Zheng, Q. Li, Dynamically actuated soft heliconical architecture via frequency of electric fields, Nat. Comm. 13 (2022) 2712.

[20] J.-D. Lin, Y.-S. Zhang, J.-Y. Lee, T.-S. Mo, H.-C Yeh, C.-R. Lee, Electrically tunable liquid-lrystal–polymer composite laser with symmetric sandwich structure, Macromolecules 53 (2020) 913–921.

[21] R.J. Mandle, S.J. Cowling, J.W. Goodby, A nematic to nematic transformation exhibited by a rod-like liquid crystal, Phys. Chem. Chem. Phys. 19 (2017) 11429–11435.

[22] H. Nishikawa, K. Shiroshita, H. Higuchi, Y. Okumura, Y. Haseba, S.-I. Yamamoto, K. Sago, H. Kikuchi, A fluid liquid-crystal material with highly polar order, Adv. Mater. 29 (2017) 1702354.

[23] A. Mertelj, L. Cmok, N. Sebastián, R.J. Mandle, R.R. Parker, A.C. Whitwood, J.W. Goodby, M. Čopič, Splay nematic phase, Phys. Rev. X 8 (2018) 041025.

[24] R.J. Mandle, A. Mertelj, Orientational order in the splay nematic ground state, Phys. Chem. Chem. Phys. 21 (2019) 18769–18772.

[25] N. Sebastián, L. Cmok, R.J. Mandle, M.R. de la Fuente, I. Drevenšek Olenik, M. Čopič, A. Mertelj, Ferroelectric-Ferroelastic phase transition in a nematic liquid crystal, Phys. Rev. Lett. 124 (2020) 37801.

[26] P.L.M. Connor, R.J. Mandle, Chemically induced splay nematic phase with micron scale periodicity, Soft Matter 16 (2020) 324–329.

[27] X. Chen, E. Korblova, D. Dong, X. Wei, R. Shao, L. Radzihovsky, M.A. Glaser, J.E. Maclennan, D. Bedrov, D.M. Walba, N.A. Clark, First-principles experimental demonstration of ferroelectricity in a thermotropic nematic liquid crystal: polar domains and striking electro-optics, Proc. Natl. Acad. Sci. U.S.A. 117 (2020) 14021–14031.

[28] O.D. Lavrentovich, Ferroelectric nematic liquid crystal, a century in waiting, Proc. Natl. Acad. Sci. U.S.A. 117 (2020) 14629–14631.

[29] X. Chen, E. Korblova, M.A. Glaser, J.E. Maclennan, D.M. Walba, N.A. Clark, Polar in-plane surface orientation of a ferroelectric nematic liquid crystal: polar monodomains and twisted state electro-optics, Proc. Natl. Acad. Sci. U.S.A. 118 (2021) e2104092118.

[30] J. Etxebarria, C.L. Folcia, J. Ortega, Generalization of the Maier-Saupe theory to the ferroelectric nematic phase, Liq. Cryst. 49 (2022) 1719–1724.

[31] A. Manabe, M. Bremer, M. Karska, Ferroelectric nematic phase at and below room temperature, Liq. Cryst. 48 (2021) 1079–1086.

[32] J. Li, H. Nishikawa, J. Kougo, J. Zhou, S. Dai, W. Tang, X. Zhao, Y. Hisai, M. Huang, S. Aya, Development of ferroelectric nematic fluids with giant-ε dielectricity and nonlinear optical properties, Sci. Adv. 7 (2021) eabf5047.

[33] C.L. Folcia, J. Ortega, R. Vidal, T. Sierra, J. Etxebarria, The ferroelectric nematic phase: an optimum liquid crystal candidate for nonlinear optics, Liq. Cryst. 49 (2022) 899–906.

[34] C. Feng, R. Saha, E. Korblova, D. Walba, S.M. Sprunt, A. Jakli, Electrically tunable reflection color of chiral ferroelectric nematic liquid crystals, Adv. Opt. Mater. 9 (2021) 2101230–2101238.

[35] H. Nishikawa, F. Araoka, A new class of chiral nematic phase with helical polar order, Adv. Mater. 33 (2021) 2101305–2101309.

[36] J. Ortega, C.L. Folcia, J. Etxebarria, T. Sierra, Ferroelectric chiral nematic liquid crystals: new photonic materials with multiple bandgaps controllable by low electric fields, Liq. Cryst. 49 (2022) 2128–2136.

[37] X. Zhao, J. Zhou, J. Li, J. Kougo, Z. Wan, M. Huang, S. Aya, Spontaneous helielectric nematic liquid crystals:electric analog to helimagnets, Proc. Natl. Acad. Sci. U.S.A. 118 (2021) e2111101118.

[38] D. Pociecha, R. Walker, E. Cruickshank, J. Szydlowska, P. Rybak, A. Makal, J. Matraszek, J.M. Wolska, J.M.D. Storey, C.T. Imrie, E. Gorecka, Intrinsically chiral ferronematic liquid crystals: an inversion of the helical twist sense at the chiral nematic – Chiral ferronematic phase transition, J. Mol. Liq. 361 (2022) 119532–119535.

[39] S. Aya, H. Xu, H. Long, M. Yiliu, Y. Zou, M. Huang, Response of helielectric nematics under an in-plane electric field, Phys. Chem. Chem. Phys. 26 (2024) 12422–12432.

[40] G. Sanz-Enguita, J. Ortega, C.L. Folcia, I. Aramburu, J. Etxebarria, Role of sample thickness on the performance of cholesteric liquid crystal lasers: experimental, numerical, and analytical results, J. Appl. Phys. 119 (2016) 073102.

[41] J. Etxebarria, J. Ortega, C.L. Folcia, G. Sanz-Enguita, I. Aramburu, Thermally induced light-scattering effects as responsible for the degradation of cholesteric liquid crystal lasers, Opt. Lett. 40 (2015) 1262–1265.

[42] Y. Takanishi, Y. Ohtsuka, G. Suzaki, S. Nishimura, H. Takezoe, Low threshold lasing from dye-doped cholesteric liquid crystal multi-layered structures, Opt. Express 18 (2010) 12909–12914.

[43] J. Ortega, C.L. Folcia, J. Etxebarria, Laser emission at the second-order photonic band gap in an electric-field-distorted cholesteric liquid crystal, Liq. Cryst. 46 (2019) 2159–2166.